The distribution of calbindin-D28k, parvalbumin, and calretinin immunoreactivity in the inferior colliculus of circling mouse

Jin-Koo Lee[1], Myeung Ju Kim[2]

Departments of [1]Pharmacology and [2]Anatomy, Dankook University College of Medicine, Cheonan, Korea

Abstract: The circling mice with *tmie* gene mutation are known as an animal deafness model, which showed hyperactive circling movement. Recently, the reinvestigation of circling mouse was performed to check the inner ear pathology as a main lesion of early hearing loss. In this trial, the inner ear organs were not so damaged to cause the hearing deficit of circling (cir/cir) mouse at 18 postnatal day (P18) though auditory brainstem response data indicated hearing loss of cir/cir mice at P18. Thus, another mechanism may be correlated with the early hearing loss of cir/cir mice at P18. Hearing loss in the early life can disrupt the ascending and descending information to inferior colliculus (IC) as integration site. There were many reports that hearing loss could result in the changes in Ca^{2+} concentration by either cochlear ablation or genetic defect. However, little was known to be reported about the correlation between the pathology of IC and Ca^{2+} changes in circling mice. Therefore, the present study investigated the distribution of calcium-binding proteins (CaBPs), calbindin-D28k, parvalbumin, and calretinin immunoreactivity (IR) in the IC to compare among wild-type (+/+), heterozygous (+/cir), and homozygous (cir/cir) mice by immunohistochemistry. The decreases of CaBPs IR in cir/cir were statistically significant in the neurons as well as neuropil of IC. Thus, this study proposed overall distributional alteration of CaBPs IR in the IC caused by early hearing defect and might be helpful to elucidate the pathology of central auditory disorder related with Ca^{2+} metabolism.

Key words: Circling mice, Calbindin-D28k, Parvalbumins, Calretinin, Inferior colliculus

Introduction

The circling mouse is one of the deafness animal model due to spontaneous mutation of the transmembrane inner ear (*tmie*) gene [1]. The homozygote (cir/cir) mouse continues hyperactive circling movement with head tossing at about 7 postnatal day (P) as the name suggests [2, 3]. However, the reinvestigation of cochlear and spiral ganglion pathology in cir/cir mouse, which were previously known as main lesions of the deafness caused by genetic defect [3], were performed recently [4]. They suggested that the impairment of both the spiral ganglion and cochlear were not significantly responsible for the hearing deficit of cir/cir mice at P18 though auditory brainstem response results were hearing loss in P18 cir/cir mice. Thus, the hearing loss did not seem to depend exclusively on the peripheral deafferentation but are, at least not entirely, of central origin. In addition, another underlying mechanism such as neurotransmitters or ion movement disorder may closely correlate with the early hearing loss of cir/cir mice.

The maintenance of structural and functional integrity of the neurons in auditory brainstem circuit is critically significant since the loss of cochlear integrity by cochlear abla-

Corresponding author:
Myeung Ju Kim
Department of Anatomy, Dankook University College of Medicine, 119 Dandae-ro, Dongnam-gu, Cheonan 31116, Korea
Tel: +82-41-550-3853, Fax: +82-41-550-3866, E-mail: mjukim99@dankook.ac.kr

tion has resulted in various morphological, biochemical, and metabolic changes throughout the auditory pathway [5, 6]. Auditory brain stem along with superior olivary nucleus and cochlear nuclear complex possesses distinct activity properties that process both ascending and descending auditory information. Hearing loss induced by unilateral/bilateral cochlear ablation in neonatal rat pups has been reported to disrupt the development of afferent projections from the dorsal nucleus of lateral leminiscus to the central nucleus of inferior colliculus (ICC) [7, 8].

The inferior colliculus (IC) occupies a strategic position in the central auditory system, which is located in the midbrain and receives input from virtually all the lower brainstem nuclei in the auditory pathway [9], as well as inputs from the auditory cortex [10]. IC processes the filtering of the self-effected sounds such as respiration, chewing, or vocalization activities and strategic integration site in auditory pathway receiving inhibitory and excitatory afferents from the majority of brainstem nuclei [11, 12]. The IC can be subdivided into three major parts as the central nucleus, a dorsal IC (DC) cortex, and a lateral IC cortex [13]. Almost all of the ascending auditory fibers end in orderly tonotopic array of fibrodendritic lamina of ICC [14], which send to the ventral subdivision of the medial geniculate body and subsequently to the auditory cortex [15]. Fibrodendritic laminae and synaptic connections are overlapped and subdivided ICC into functional areas [10]. In contrast to ICC, IC cortices consist of several functional layers with separate input and output connections [9].

The regulation of calcium (Ca^{2+}) concentrations is critical for the synaptic function and plasticity in the central nervous system [16]. In addition, previous study linked Ca^{2+} disturbances directly with hearing loss [17]. For the proper functioning of the auditory neurons and cochlear hair cells, the regulation of Ca^{2+} concentration should be performed competently by active transportation of Ca^{2+} via calcium-binding proteins (CaBPs) [18]. CaBPs such as calbindin-D28k (CB), parvalbumin (PV), and calretinin (CR) act as buffers for maintaining Ca^{2+} homeostasis in numerous processes [19]. However, it is not well established how CB, PV, and CR proteins act in the central auditory system such as the IC. Moreover, there is few studies in hearing loss to address the effect on the calcium binding proteins distribution in the inferior colliculus, especially with regard to genetic defect mice.

Therefore, the present study investigates the distribution of CB, PV, and CR in the IC by using immunohistochemistry to compare CB, PV, and CR immunoreactivities (IRs) between wild-type (+/+), heterozygous (+/cir), and homozygous (cir/cir) mice.

Materials and Methods

Animals

Fifteen mice (+/+, n=5; +/cir, n=5; and cir/cir, n=5) were used in the present study. The mice were kept under controlled conditions (ambient temperature of 20°C–25°C, 12-hour light/dark cycle). Food (Samtako Bio Korea, Osan, Korea) and water were supplied *ad libitum*. The animals were maintained in the Laboratory Animal Research Center of the Dankook University (DKU). National Institutes of Health (NIH) guidelines of animal research was followed for all animal procedures and was approved by the Dankook University Institutional Animal Care and Use Committee (DUIAC), which adheres to the guidelines issued by the Institution of Laboratory of Animal Resources. Postnatal day 16 (P16) heterozygote (+/cir) and homozygote (cir/cir) circling mice were obtained from the mating of cir/cir males with +/cir females. To prevent genetic mixings, both +/cir and cir/cir mice were completely separated from wild-type (+/+) mice, which were purchased from the laboratory animal company (Samtako Bio Korea). Polymerized chain reaction analysis was performed to differentiate +/cir and cir/cir mice using genomic DNA obtained from mouse-tails. The genomic DNA was isolated according to the manufacturer's instructions (Bioneer, Daejeon, Korea). The cir/cir mouse was identified by absence of the *tmie* gene [3].

Immunohistochemistry

Mice were deeply anesthetized and perfused transcardially with cold phosphate buffer (0.1 M phosphate buffered saline [PBS, pH 7.4]), followed by cold 4% paraformaldehyde (PFA) in 0.1M PBS. The brains were post-fixed in PFA for 24 hours, then cryoprotected in a series of sucrose solutions (10%, 20%, and 30%) in PBS at 4°C. Immunohistochemistry was performed in accordance with the free-floating method described earlier [20]. Briefly, serial cryostat sections (40 μm thick) in the coronal plane were used for immunohistochemical staining with polyclonal anti-rabbit CB (AB1778, Millipore, Temecula, CA, USA), polyclonal anti-rabbit PV (PV 25, Swant, Bellinzona, Switzerland), and polyclonal anti-goat CR (AB1550, Millipore) antibodies. The antibodies were applied to brain sections at the dilution ratios of 1:5,000, 1:10,000, and

1:15,000, respectively in blocking buffer (2% bovine serum albumin, 0.3% Triton X-100, 1% horse serum, and 0.1 M PBS). The sections were incubated for 48 hours at 4°C. The sections were washed 3 times for 15 minutes each in PBS, incubated in biotinylated anti-rabbit and -goat IgG as a dilution ratio of 1:250 at room temperature for 1.5 hours, and washed again 3 times for 15 minutes each in PBS. Sections were then treated with an avidin-biotin-peroxidase complex (Vectastatin ABC mouse Elite kit, Vector Laboratories, Burlingame, CA, USA) following the manufacturer's manual. The reaction was visualized using a solution containing 0.05% diaminobenzidine and 0.015% hydrogen peroxide. Sections were mounted on gelatin-coated slides, dehydrated, and cover-slipped. Sections from each group were stained together to eliminate conflicts between different experimental conditions. Omission of the primary antiserum served as a negative control.

Image analysis

The stained sections were examined using an Olympus BX51 microscope and pictures of the sections were captured with a microscope digital camera system (BX51, Olympus, Tokyo, Japan). The IC areas were identified based on the atlas of the mouse brain [21]. The NIH image program (Scion Image, Bethesda, MD, USA) was used to determine staining densities, as described previously [20]. The sum of the gray values of all pixels in each corresponding regions was divided by the total number of pixels in the region to determine the mean density of IR per unit area (mm^{-2}). Investigator performing the analysis of the slides was blinded to the classification of the three types.
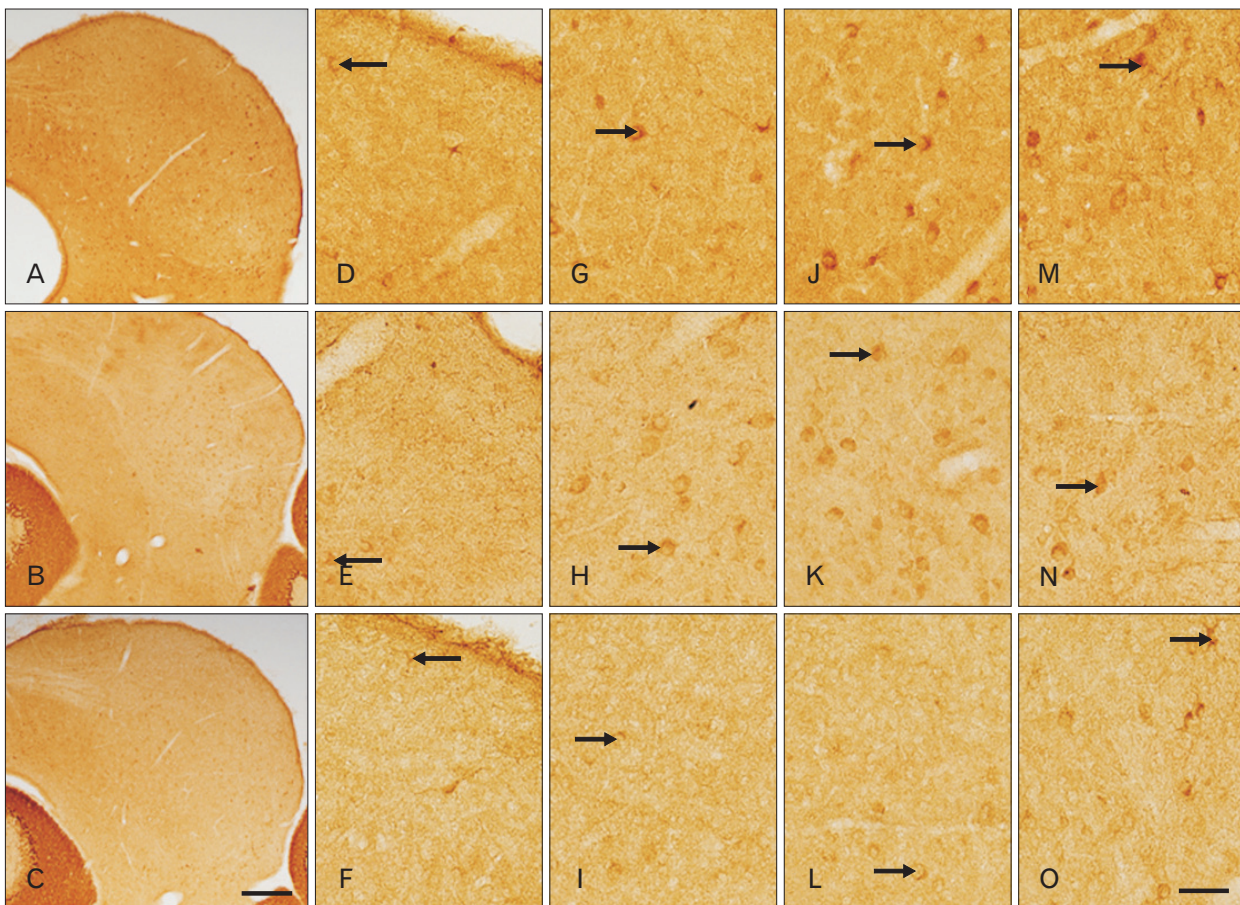
Fig. 1. Distribution of calbindin-D28k (CB) immunoreactivity (IR) in coronal sections through the inferior colliculus (IC) of postnatal day 16 wild-type (+/+) (A, D, G), heterozygous (+/cir) (B, E, H), and homozygous (cir/cir) (C, F, I) mice. CB IR was noted to be drastically decreased in both +/cir and cir/cir as compared with +/+ in the whole IC region. Prominent loss of staining was noted in the cells (arrows) of both outer dorsal cortex of IC (DC) and inner DC of cir/cir (D–I). Oval to round in shape cells (arrows) with very short proximal dendritic staining along with immunoreactive fibers were noted in the central nucleus of IC region (J–L). Loss of such cells and fibers were noted in cir/cir. The lateral nucleus of IC region consisted of oblong, stellate and oval soma (arrows) which were darkly stained in +/+ but was very faint in +/cir and cir/cir (M–O). Scale bars=100 μm (A–C), 50 μm (D–O).

Statistical analysis

The results were expressed as mean±SD. Comparison of the mean density of IC of +/+ with +/cir and cir/cir mice respectively. The analysis was done individually by Student's *t* test using SPSS software version 14 (SPSS Inc., Chicago, IL, USA). *P*-value less than 0.05 was considered to be statistically significant.

Results

CB IR

The CB IR in the IC revealed the CB cells to be more numerous in the ICC but few in dorsal cortex of IC (DC) and the lateral nucleus of IC (LN) with general distribution of neuropil staining in all the three types (Fig. 1). The CB IR was noted to decrease drastically in the whole IC region of +/cir and cir/cir as compared with +/+. The outer layer of DC in +/+ revealed few CB immunoreactive cells along with CB immunoreactive fibers while the inner layer of DC comprised of numerous oval and stellate shaped cells (Fig. 1G-L). The cells in the DC of +/cir appeared to be less darkly stained as compared with +/+ while DC of cir/cir revealed a prominent loss of IR in the cells (Fig. 1G-L).

CB immunoreactive cells in the ICC of +/+ appeared to be oval to round in shape with very short proximal dendritic staining (Fig. 1J-L). Immunoreactive fibers were also noted which could probably be lemniscal tract that are CB immunoreactive. The CB immunoreactive cells of +/cir appeared to
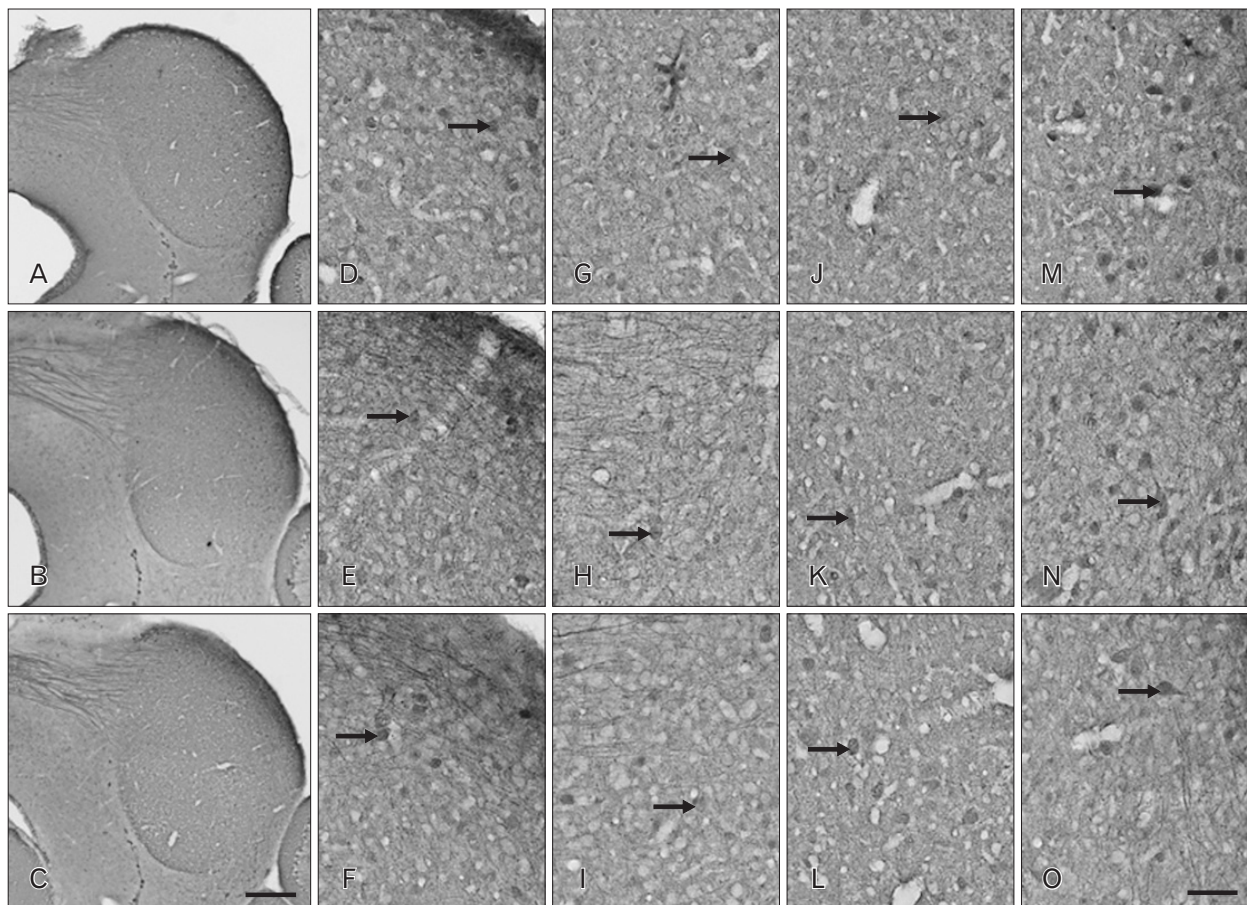
Fig. 2. Distribution of parvalbumin (PV) immunoreactivity (IR) in coronal sections through the inferior colliculus (IC) of postnatal day 16 wild-type (+/+) (A, D, G), heterozygous (+/cir) (B, E, H), and homozygous (cir/cir) (C, F, I) mice. PV IR was distributed with varying intensity which was slightly lower in cir/cir and the labeling intensity was noted to be highest in the dorsolateral part of IC. Oval to multipolar cells (arrows) were stained in both the outer dorsal cortex of IC (DC) and inner DC region (D–I). Numerous PV immunoreactive cells (arrows) were also present in the central nucleus of IC region of all the three types which appeared to be oval, spindle and multipolar in shape (J–L). Lateral nucleus of IC region consisted of cells (arrows) displaying proximal dendritic staining and immunoreactive fibers as well (M–O). Scale bars=100 μm (A–C), 50 μm (D–O).

lightly stained as compared with +/+. ICC of cir/cir showed loss of CB reactivity while some of the cells appeared to be unstained (Fig. 1L).

Darkly stained CB immunoreactive cells with oblong, stellate and oval soma were observed in the LN of +/+ (Fig. 1M-O). The LN of +/cir and cir/cir also displayed CB immunoreactive cells but were very faintly stained as compared with +/+ (Fig. 1O). Along with cells, few CB immunoreactive fibers were also perceived which appeared to run parallel to the surface of LN.

PV IR

PV IR was detected to be distributed throughout the subdivisions of IC in all the three types with varying intensity. Overall slight decrease in IR was noted in cir/cir as compared with +/+ and +/cir (Fig. 2). Majority of the PV immunoreactive cells as well as the staining intensity appeared to be highest in the dorsolateral part of IC (Fig. 2A-C). Oval to multipolar shaped neurons as well as neuropil appeared to be stained distinctly in the DC of IC in both the outer and inner layer (Fig. 2D-I). PV immunoreactive fibers were also noted which were more prominent in +/cir and cir/cir than +/+.

Numerous darkly stained PV immunoreactive cells were
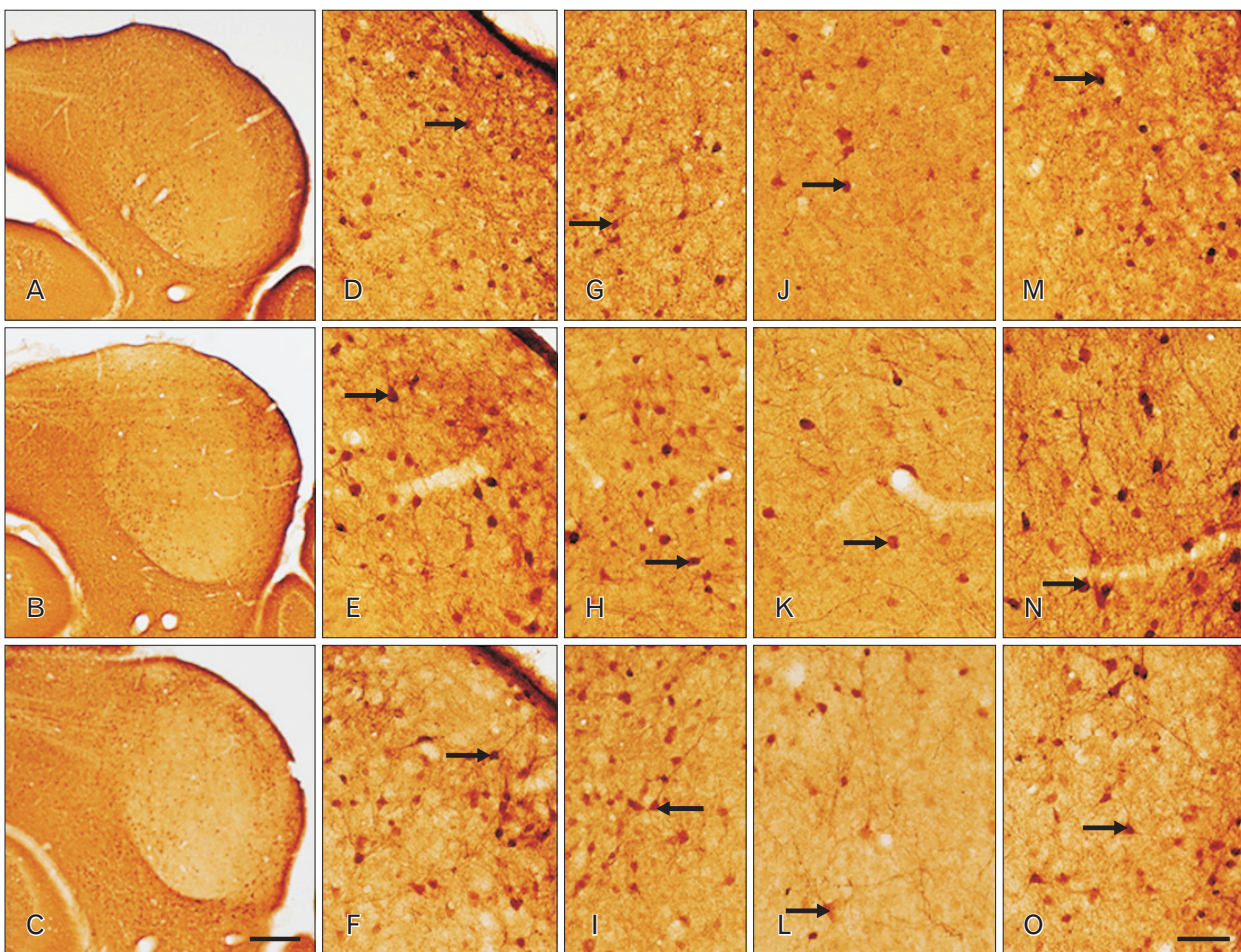
Fig. 3. Distribution of calretinin (CR) immunoreactivity (IR) in coronal sections through the inferior colliculus (IC) of postnatal day 16 wild-type (+/+) (A, D, G), heterozygous (+/cir) (B, E, H), and homozygous (cir/cir) (C, F, I) mice. Highly stained cells were noted in dorsal cortex of IC (DC) and lateral nucleus of IC (LN) region but were very less in central nucleus of IC (ICC) of all the three types with varying intensity. Flattened cells (arrows) with dendrites sprouting out was observed in the outer DC (D–F) while the inner DC consisted of triangular, rounded or occasionally round shaped cells (arrows) (G–I). Diffuse background staining of neuropil prominent in +/+ was lacking in cir/cir. lightly stained cells (arrows) and diffuse neuropil staining was noted in ICC which decreased prominently in cir/cir (J–L). CR immunoreactive lemniscal tract fibers were also present. Numerous CR positive cells (arrows) with dendrites running parallel to the surface of IC along with immunoreactive fibers were noted in the LN region (M–O). CR IR in cells, fibers, and neuropil appeared to be prominently decrease in all the regions of IC of cir/cir as compared with +/+. Scale bars=100 μm (A–C), 50 μm (D–O).

noted to be scattered in the ICC of +/+ and +/cir but was slightly lighter in cir/cir, although no difference in number of cell was observed (Fig. 2J–L). Such PV immunoreactive cells were spindle, multipolar as well as oval in shape. Distinctly PV immunoreactive cells and fibers were observed in the LN (Fig. 2M–O). The cells were mainly oval shaped with proximal dendritic staining. The immunoreactive fibers appeared to run parallel to the LN surface. Comparison between the three types showed slight decrease in PV IR in the cells as well as the neuropil of cir/cir (Fig. 2A–C).

CR IR

The general staining pattern of CR IR in the IC revealed large number of immunoreactive cells in the DC as well as in the LN but was almost absent in the ICC region (Fig. 3). Overall the staining pattern appeared to reveal a decrease in IR in cir/cir as compared with +/+. Darkly stained cells were noted in the different layers of DC with varying intensity in all the three types (Fig. 3D–I). The outer layer of DC consisted of few flattened cells with dendrites sprouting out in all the three types. Inner layer of DC revealed evenly distributed cells, which were triangular, rounded or occasionally rounded in shape (Fig. 3G–I). Such CR immunoreactive cells of cir/cir displayed lighter staining as compared with +/+. Diffuse background staining of neuropil was noted in DC, which was lacking in cir/cir but very much prominent in +/+ and +/cir (Fig. 3D–I).

The ICC in all the three types displayed few lightly stained cells and diffuse neuropil staining in all the three types (Fig. 3J–L). The staining intensity of such CR immunoreactive cells and the neuropil appeared to decrease prominently in cir/cir when compared with +/+ (Fig. 3J, L). The cells appeared to be almost devoid of IR. Occasional CR immunoreactive lemniscal tract fibers were also present whose staining intensity was severely decreased in cir/cir.

The LN of IC comprised of numerous CR immunoreactive cells with dendrites running parallel to the surface of the IC. The cells were oval or pyramidal in shape (Fig. 3M–O). Highly immunoreactive fibers and neuropil was also noted running along the surface of LN. This layer could be continuous with the outer layer of DC. Such CR IR in cells, fibers and neuropil appeared to be decreased in cir/cir while +/+ and +/cir were prominently stained (Fig. 3M–O).

Statistical analysis of CaBPs IR

CB IR

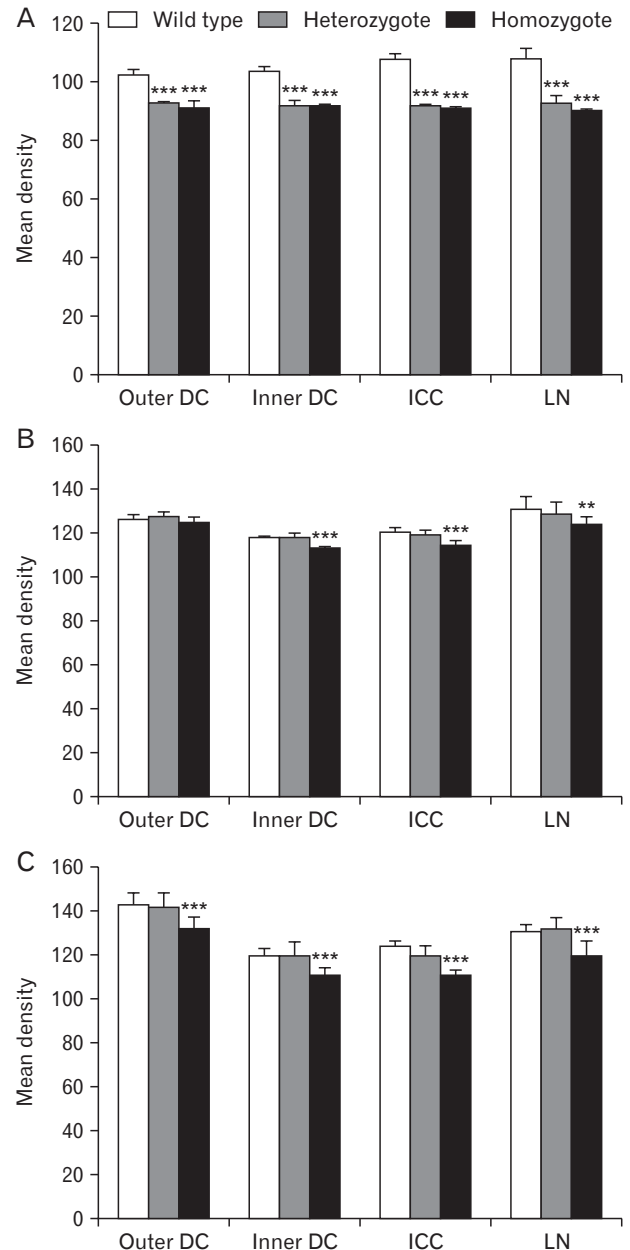Image analysis assessment of the ICC revealed a significant

Fig. 4. Image analysis of relative density of calbindin-D28k (A), parvalbumin (B), and calretinin (C) immunoreactivity (IR) changes in the inferior colliculus (IC) of postnatal day 16 wild-type (+/+), heterozygous (+/cir), and homozygous (cir/cir) mice. Decrease in the IR was noted in cir/cir in the various different regions of IC as compared with +/+. The data shown are the mean±SD obtained from three different experiments. DC, dorsal cortex of IC; ICC, central nucleus of IC; LN, lateral nucleus of IC. **$P<0.01$, ***$P<0.001$, compared with wild-type.

difference in the relative mean density of CB IR in +/cir and cir/cir when compared with +/+. Comparison between all the parts (outer DC, inner DC, ICC, and LN) of IC of +/+ with +/cir revealed significant difference ($P<0.001$) (Fig. 4A). Similarly, the difference parts (DC, ICC, and LN) of IC of cir/cir also showed significant difference ($P<0.001$) when compared with +/+ (Fig. 4A).

PV IR

PV IR assessment by image analysis in the different parts of IC revealed the relative mean density to be highest level in +/+ and lowest in cir/cir. Comparison within the different parts of the IC showed highest IR to be present in the LN region and lowest in the inner DC of all the three types. PV IR was observed to be significantly lower in inner DC ($P<0.001$), ICC ($P<0.001$), and LN ($P<0.01$) of cir/cir than those of +/+ (Fig. 4B). No significant difference was noted in the outer DC of cir/cir and all the parts of IC of +/cir as compared with +/+ (Fig. 4B).

CR IR

PV IR assessment by image analysis performed to measure the CR IR in the IC noted highest level in the outer DC followed by LN, ICC, and inner DC, respectively of all the three types. Comparison between groups revealed highest CR IR in the +/+ and lowest in cir/cir (Fig. 4C). Compared with +/+, cir/cir showed significant changes in all the fields of IC ($P<0.001$) (Fig. 4C). But, no significant difference was noted in the CR IR in the IC fields of +/cir when compared with +/+ (Fig. 4C).

Discussion

IC as a major brain stem auditory relay nucleus participates in more complex aspects of auditory processing like attention [22]. The neuron's activity relation with CaBPs have been noted to susceptibility to calcium-dependent pathologies in of the auditory system [23]. CB staining in the IC has been reported in various mammals including rat [24-26], bat [27], chinchilla [28], and mice [29]. In general, the CB IR in IC of +/+ resembled that of CBA/CaJ and C57Bl/6 mice [29] in that the CB immunoreactive cells appeared to be scattered throughout the IC. In contrast to the present finding, the ICC region in rat either was devoid of CB immunoreactive cells [24, 26] or had very few lightly labeled CB immunoreactive cells [25]. Unlike present study, the cells in IC of rat were

more abundant in the DC [24, 26]. As compared with +/+, the prominent loss of CB IR in all the IC regions of both +/cir and cir/cir was noticeable. Decrease in CB immunoreactive cells has been noted in deaf mice [29]. Increase in CB IR has been reported in IC after sound stimulation hinting to the possible protective role as Ca^{2+} buffers in response to increased intracellular Ca^{2+}. Considering the neuroprotective role of CB, decrease in CB IR could be hinting to an increased susceptibility to Ca^{2+}-dependent pathologies especially in the auditory system of cir/cir. Substantial loss of CB immunoreactive cells in cir/cir might also be contributed to the hearing loss in cir/cir.

General architecture of PV IR in IC for the present study appears to be remarkably similar with studies conducted in rat [30], human [31], cat [32], and mice [33] with slight variation in the distribution of the cells. Present study noted the PV immunoreactive to be distributed in all parts of IC but was more concentrated in the ventrolateral part, which is in agreement with p12 rat [30]. Unstained dendrites observed in the DC and ICC is in agreement with previous studies [32, 34] but does not agree with the dendritic staining observed in the LN of all the three types. PV immunoreactive neurons in the IC have been reported to be GABAergic as well [32, 35]. Decrement of the PV IR in the IC as in cir/cir could lead to loss of innervation of the GABAergic neurons as reported in previous studies. Moreover, the loss of PV IR in neurons as well as neuropil has been reported in other location of brain as well as IC, leading to substantial deterioration of hearing function [36].

The CR IR pattern of the present study is similar to that in rat [26, 30] and mice [29], in that the ICC is almost devoid of CR immunoreactive cells but presents CR immunoreactive fibers. Heavy existence of CR immnunoreactive cells in the DC and LN parts of all the three types is in agreement with study in CBA/CaJ and C57Bl/6 mice [29] but differs from those reported in rats [30]. Early bilateral deafening has been reported to prevent age related increase of CR immunostained cells [37]. Unilateral cochlear ablation at the onset time of hearing also reported CR upregulation only in the IC contralateral to the lesion, which further supports the study. Consistent with those findings the present study also noted a decrease in the CR IR in the IC of cir/cir, which might be contributed to deafness induced by the pathological features in cochlea. These findings suggest CR upregulation to be mediated by sound-evoked activity from cochlear input. Alteration in the CR IR intensity in cir/cir could be the result of disturbance

in neuronal Ca^{2+} homeostasis mechanism, which could lead to modification in intracellular Ca^{2+} level affecting neuronal processes such as neurotransmitter release. This is supported by previous study reported disturbance in the release of glutamate and glycine in cir/cir [38]. In the IC, age-related changes in its volume, neuron number, neuron size, or packing density were examined on both C57BL/6J and CBA/J mice, but there was no statistically significant difference [39]. Thus, the changes we observed are likely to be the result of hearing loss associated with the expressional alterations of these calcium-binding proteins in existing cell populations, rather than reflecting the changes of total cell number.

Taken together, the cir/cir mice showing profound hearing loss early in life could be susceptible to Ca^{2+} dependent detrimental effects as shown in prominent decreases of CaBPs IR in cir/cir and might be more vulnerable to calcium related degeneration in auditory system. These data might be helpful to elucidate the hearing defect related with the susceptibility to calcium-dependent pathology.

Acknowledgements

References

1. Shin MJ, Lee JH, Yu DH, Kim BS, Kim HJ, Kim SH, Kim MO, Park C, Hyun BH, Lee S, So HS, Park R, Ryoo ZY. Ectopic expression of tmie transgene induces various recovery levels of behavior and hearing ability in the circling mouse. Biochem Biophys Res Commun 2008;374:17-21.

2. Cho KI, Lee JW, Kim KS, Lee EJ, Suh JG, Lee HJ, Kim HT, Hong SH, Chung WH, Chang KT, Hyun BH, Oh YS, Ryoo ZY. Fine mapping of the circling (cir) gene on the distal portion of mouse chromosome 9. Comp Med 2003;53:642-8.

3. Chung WH, Kim KR, Cho YS, Cho DY, Woo JH, Ryoo ZY, Cho KI, Hong SH. Cochlear pathology of the circling mouse: a new mouse model of DFNB6. Acta Otolaryngol 2007;127:244-51.

4. Lee Y, Chang SY, Jung JY, Ahn SC. Reinvestigation of cochlear pathology in circling mice. Neurosci Lett 2015;594:30-5.

5. Illing RB. Activity-dependent plasticity in the adult auditory brainstem. Audiol Neurootol 2001;6:319-45.

6. Syka J. Plastic changes in the central auditory system after hearing loss, restoration of function, and during learning. Physiol Rev 2002;82:601-36.

7. Franklin SR, Brunso-Bechtold JK, Henkel CK. Unilateral co-

8. Franklin SR, Brunso-Bechtold JK, Henkel CK. Bilateral cochlear ablation in postnatal rat disrupts development of banded pattern of projections from the dorsal nucleus of the lateral lemniscus to the inferior colliculus. Neuroscience 2008;154:346-54.

9. Ito T, Hirose J, Murase K, Ikeda H. Determining auditory-evoked activities from multiple cells in layer 1 of the dorsal cortex of the inferior colliculus of mice by in vivo calcium imaging. Brain Res 2014;1590:45-55.

10. Ono M, Ito T. Functional organization of the mammalian auditory midbrain. J Physiol Sci 2015;65:499-506.

11. Irvine DR. Physiology of the auditory brainstem. In: Popper AN, Fay RR, editors. The Mammalian Auditory Pathway: Neurophysiology. New York: Springer; 1992. p.153-231.

12. Oliver DL, Huerta MF. Inferior and superior colliculi. In: Webster DB, Popper AN, Fay RR, editors. The Mammalian Auditory Pathway: Neuroanatomy. New York: Springer; 1992. p.168-221.

13. Patel MB, Sons S, Yudintsev G, Lesicko AM, Yang L, Taha GA, Pierce SM, Llano DA. Anatomical characterization of subcortical descending projections to the inferior colliculus in mouse. J Comp Neurol 2017;525:885-900.

14. Shneiderman A, Henkel CK. Banding of lateral superior olivary nucleus afferents in the inferior colliculus: a possible substrate for sensory integration. J Comp Neurol 1987;266:519-34.

15. Shneiderman A, Oliver DL, Henkel CK. Connections of the dorsal nucleus of the lateral lemniscus: an inhibitory parallel pathway in the ascending auditory system? J Comp Neurol 1988;276:188-208.

16. German DC, Manaye KF, Sonsalla PK, Brooks BA. Midbrain dopaminergic cell loss in Parkinson's disease and MPTP-induced parkinsonism: sparing of calbindin-D28k-containing cells. Ann N Y Acad Sci 1992;648:42-62.

17. Mammano F. Ca^{2+} homeostasis defects and hereditary hearing loss. Biofactors 2011;37:182-8.

18. Tong B, Hornak AJ, Maison SF, Ohlemiller KK, Liberman MC, Simmons DD. Oncomodulin, an EF-hand Ca2+ Buffer, is critical for maintaining cochlear function in mice. J Neurosci 2016;36:1631-5.

19. Yew DT, Luo CB, Heizmann CW, Chan WY. Differential expression of calretinin, calbindin D28K and parvalbumin in the developing human cerebellum. Brain Res Dev Brain Res 1997;103:37-45.

20. Maskey D, Pradhan J, Kim HJ, Park KS, Ahn SC, Kim MJ. Immunohistochemical localization of calbindin D28-k, parvalbumin, and calretinin in the cerebellar cortex of the circling mouse. Neurosci Lett 2010;483:132-6.

21. Paxinos G, Franklin KB. The mouse brain in stereotaxic coordinates. 2001. San Diego, CA: Academic Press; 2001.

22. Hoormann J, Falkenstein M, Hohnsbein J. Effect of selective attention on the latency of human frequency-following potentials. Neuroreport 1994;5:1609-12.

23. Idrizbegovic E, Bogdanovic N, Willott JF, Canlon B. Age-related

increases in calcium-binding protein immunoreactivity in the cochlear nucleus of hearing impaired C57BL/6J mice. Neurobiol Aging 2004;25:1085-93.

24. Celio MR. Calbindin D-28k and parvalbumin in the rat nervous system. Neuroscience 1990;35:375-475.

25. Friauf E. Distribution of calcium-binding protein calbindin-D28k in the auditory system of adult and developing rats. J Comp Neurol 1994;349:193-211.

26. Rogers JH, Résibois A. Calretinin and calbindin-D28k in rat brain: patterns of partial co-localization. Neuroscience 1992;51:843-65.

27. Zettel ML, Carr CE, O'Neill WE. Calbindin-like immunoreactivity in the central auditory system of the mustached bat, Pteronotus parnelli. J Comp Neurol 1991;313:1-16.

28. Kelley PE, Frisina RD, Zettel ML, Walton JP. Differential calbindin-like immunoreactivity in the brain stem auditory system of the chinchilla. J Comp Neurol 1992;320:196-212.

29. Zettel ML, Frisina RD, Haider SE, O'Neill WE. Age-related changes in calbindin D-28k and calretinin immunoreactivity in the inferior colliculus of CBA/CaJ and C57Bl/6 mice. J Comp Neurol 1997;386:92-110.

30. Lohmann C, Friauf E. Distribution of the calcium-binding proteins parvalbumin and calretinin in the auditory brainstem of adult and developing rats. J Comp Neurol 1996;367:90-109.

31. Tardif E, Chiry O, Probst A, Magistretti PJ, Clarke S. Patterns of calcium-binding proteins in human inferior colliculus: identification of subdivisions and evidence for putative parallel systems. Neuroscience 2003;116:1111-21.

32. Paloff AM, Usunoff KG, Yotovski P, Hinova-Palova DV, Ovtscharoff WA. Parvalbumin-like immunostaining in the cat inferior colliculus: light and electron microscopic investigation. Acta Histochem 2004;106:219-34.

33. Idrizbegovic E, Bogdanovic N, Canlon B. Sound stimulation increases calcium-binding protein immunoreactivity in the inferior colliculus in mice. Neurosci Lett 1999;259:49-52.

34. Vater M, Braun K. Parvalbumin, calbindin D-28k, and calretinin immunoreactivity in the ascending auditory pathway of horseshoe bats. J Comp Neurol 1994;341:534-58.

35. Winer JA, Saint Marie RL, Larue DT, Oliver DL. GABAergic feedforward projections from the inferior colliculus to the medial geniculate body. Proc Natl Acad Sci U S A 1996;93:8005-10.

36. Ouda L, Druga R, Syka J. Changes in parvalbumin immunoreactivity with aging in the central auditory system of the rat. Exp Gerontol 2008;43:782-9.

37. Zettel ML, O'Neill WE, Trang TT, Frisina RD. Early bilateral deafening prevents calretinin up-regulation in the dorsal cortex of the inferior colliculus of aged CBA/CaJ mice. Hear Res 2001;158:131-8.

38. Hong SH, Kim MJ, Ahn SC. Glutamatergic transmission is sustained at a later period of development of medial nucleus of the trapezoid body-lateral superior olive synapses in circling mice. J Neurosci 2008;28:13003-7.

39. Willott JF, Bross LS, McFadden SL. Morphology of the inferior colliculus in C57BL/6J and CBA/J mice across the life span. Neurobiol Aging 1994;15:175-83.